

relative smallness of the π^-p as compared to the π^+p backward elastic cross sections at the large subenergies ($s_1 \sim 10 \text{ GeV}^2$) results in the relative depletion of the π^- with large p_L .

The K^\pm spectra.—The relation imposed by this model between fast meson secondaries and the cross section for meson-proton backward elastic scattering should be even more pronounced for the K^\pm spectra than the π^\pm spectra since the K^-p backward elastic cross section falls with increasing energy much more rapidly than that for the backward K^+p .⁷ We find that the K^- spectrum of Fig. 3(g) is described entirely by Fig. 1(c), while the K^+ spectrum in Fig. 3(f) requires Fig. 1(c) for slow mesons and Fig. 1(b) for fast mesons. The lack of fast K^- relative to K^+ is apparent in the measured spectra and is adequately described by our model.

To summarize, we have compared the quantitative predictions of a fairly restrictive inclusive multiperipheral model to the meson and proton spectra resulting from pp collisions at three momenta from 12 to 30 GeV/c. There are some discrepancies between the predictions of our model and the measured spectra that could perhaps be reduced by further adjustment of some parameters, but the results taken together suggest a consistent view of features of inclusive data in terms of two-body data.

We thank V. Chung for helpful discussions during the formative stages of this work, especially concerning the p_T^2 peaking mechanism. We also express our gratitude to J. Ball, G. Kane, G. Lynch, G. Marchesini, and M. Ross for useful

discussions.

*Work supported in part by the U. S. Atomic Energy Commission.

†Participating guest at Lawrence Radiation Laboratory, Berkeley, Calif. 94720.

¹C. W. Akerlof *et al.*, Phys. Rev. D **3**, 645 (1971).

²J. V. Allaby *et al.*, to be published.

³E. W. Anderson *et al.*, Phys. Rev. Lett. **19**, 198 (1967).

⁴L. Caneschi and A. Pignotti, Phys. Rev. Lett. **22**, 1219 (1969).

⁵G. Fox, in *High Energy Collisions—Third International Conference*, edited by C. N. Yang, J. A. Cole, M. Good, R. Hwa, and J. Lee-Franzini (Gordon and Breach, New York, 1970), p. 367.

⁶L. Anderson *et al.*, Phys. Rev. D **3**, 1536 (1971).

⁷L. Price *et al.*, Lawrence Radiation Laboratory Report No. UCRL-20000 K^+N , 1969 (unpublished).

⁸E. Berger and G. Fox, Nucl. Phys. **B26**, 1 (1971).

⁹We parametrize the backward differential cross section as $d\sigma/du = \beta^2(u)s^{2\alpha(u)-2}$, and from the experimentally measured cross sections in the energy range $3 < s < 6 \text{ GeV}^2$ (Refs. 6, 7) we determine $\alpha(0)$ to be -2.0 for π^-p , -1.3 for π^+p , and -0.25 for K^+p . The shape of $\alpha(u)$ is taken from Ref. 8.

¹⁰We find that the process of Fig. 1(c) accounts for 80% of the meson spectrum, while Fig. 1(b) gives rise to the remaining 20%. Figure 1(a) accounts for about 50% of the proton spectrum and Fig. 1(b) for the rest.

¹¹For $p_T^2 \gtrsim 1.6 \text{ GeV}^2$, where $t_1 \approx -4 \text{ GeV}^2$ and the angle of the emitted pion is greater than 60° , the simple Regge-pole representation of the two-body scattering amplitudes becomes invalid and the model undercuts the spectrum [Fig. 3(a)].

¹²We find that Fig. 1(c) also predicts a sharp p_T^2 peaking for $p_T < 0.3 \text{ GeV}/c$ at $p_L \sim 0$.

$\bar{K}N$ Interaction in the Region 0 to 1200 MeV/c and Hyperon Resonances*

Jae Kwan Kim

Department of Physics, Harvard University, Cambridge, Massachusetts 02139

(Received 28 March 1971)

A multichannel phase-shift analysis has been performed for the first time on the available experimental data of all the channels of $\bar{K}N$ interactions in the momentum region 0 to 1200 MeV/c. The Argand diagrams of the reaction amplitudes and the resonance parameters within the momentum region are given. The results provide stronger evidence for a number of previously suggested resonances and also indicate some new possible resonances.

The experimental data for the following reactions below the incident \bar{K} momentum of 1200 MeV/c have been accumulating very rapidly during the last five years: $\bar{K}N$ interacting into $\bar{K}N$,

$\Sigma\pi$, $\Lambda\pi$, $\bar{K}N\pi$, $\Sigma\pi\pi$, $\Lambda\pi\pi$, and $\Lambda\eta$ final channels. It has become possible to make a meaningful multichannel phase-shift analysis incorporating simultaneously the existing data of all the above

reactions at the present time.¹⁻⁸

In this first extensive multichannel phase-shift analysis covering the wide momentum region from 0 to 1200 MeV/c, the following K -matrix parametrization has been used. The energy dependence of the K matrix was parametrized by the effective-range expansion of the inverse of the K matrix due to Ross and Shaw.⁹ They defined the M matrix which is essentially the inverse of the K matrix, except for the centrifugal barrier factor,

$$K(E) = K^I M(E)^{-1} K^I.$$

The M matrix is expanded linearly in the momentum squared,

$$M(E) = M(E_0) + \frac{1}{2} r (k^2 - k_0^2),$$

where k is the diagonal matrix of the center-of-mass momenta and r is the effective-range matrix. In this analysis, the matrix r is taken to be the full matrix and it is not assumed to be diagonal as in the previous analysis.¹⁰ The scattering matrix in the Argand diagrams is given in terms of the M matrix:

$$T(E) = k^{l+1/2} [M(E) - ik^{2l+1}]^{-1} k^{l+1/2}.$$

The above expansion is essentially the linear expansion in the energy, and Ross and Shaw show that this type of expansion is similar to the Breit-Wigner multilevel resonance formula within the same limited energy region. Thus, this parametrization can allow us to detect any unknown resonances present in any partial wave and in any particular reaction channel.

Since the above linear expansion is not expected to be valid for the whole momentum region from 0 to 1200 MeV/c, the separate effective-range fits have been made for the following seven momentum intervals: 0 to 534, 534 to 658, 658 to 806, 806 to 916, 916 to 1022, 1022 to 1117, and 1117 to 1226. In doing these successive fits, only the range parameters are varied to continue the adjacent momentum intervals smoothly. The $M(E_0)$ for the next momentum interval is calculated from the $M(E)$ of the adjacent momentum-interval fit and this $M(E_0)$ is fixed. The above momentum intervals of approximately 100 MeV/c for the successive fits are decided on the basis of goodness of fit. In the preliminary result,¹¹ only S_1 , P_1 , P_3 , and D_3 waves were parametrized by the K matrix, but D_5 and F_5 waves were fixed as the known Breit-Wigner amplitudes. In this final result, all the above partial waves are parametrized by the K matrix. Thus every partial

wave is freely varied except F_{15} . This wave corresponds to the $Y_1^*(1915)$ and is fixed as the known Breit-Wigner amplitude since this resonance lies outside the momentum interval covered in this fit. The $I=0$ system is treated as the three coupled channels, $\bar{K}N$, $\Sigma\pi$, and an extra channel for the three-particle productions. The $I=1$ system is treated as the four coupled channels, $\bar{K}N$, $\Sigma\pi$, $\Lambda\pi$, and an extra channel for the three-particle productions. Thus, altogether, 86 parameters are used for the expansion-energy K -matrix elements and an additional 86 parameters are used for the r -matrix elements. For each successive expansion, only these 86 r -matrix elements are fitted. The extra parameters due to the three-particle productions were not constrained in the preliminary result mentioned above but these parameters are tightly constrained in this final result using the total three-particle production cross sections.

The experimental Legendre coefficients obtained from the available data are compared with the calculated values from the K -matrix parameters and a χ^2 function is formed using the experimental errors on the coefficients. This function is searched and minimized by using the search program MINFUM and also using the local minimizing program, STEPIT.¹² Approximately 2500 data points are fitted in this analysis. The estimate on the computer time used for this analysis is approximately 100 h of CDC 6600 and 1000 h of Sigma-7. The ratio of the χ^2 and the number of degrees of freedom is approximately 1.2 for the best solution obtained. The results of this analysis are discussed in the remainder of this Letter.

The Argand diagrams of the reaction amplitudes in the total isospin-0 channels are shown in Fig. 1. The S_{01} amplitudes resonate at the $Y_0^*(1405)$ below the $\bar{K}N$ threshold and because of this effect the amplitudes make the clockwise motion in the Argand diagram above the $\bar{K}N$ threshold. These amplitudes resonate again at 740 MeV/c and once more at 970 MeV/c. The well-known $\Lambda\pi$ resonance at 740 MeV/c with a mass 1670 MeV is strongly seen in all the channels KN , $\Sigma\pi$, and $\Lambda\eta$. The elasticity of this resonance is larger than the Berkeley table¹⁵ value and this reduces the branching ratio into the $\Lambda\eta$ channel to the much smaller value. The resonance at 970 MeV/c with a mass of 1780 MeV is highly elastic but the small loop in the $\Sigma\pi$ channel is also clearly seen. This new large elastic resonance is strongly required by the experimen-

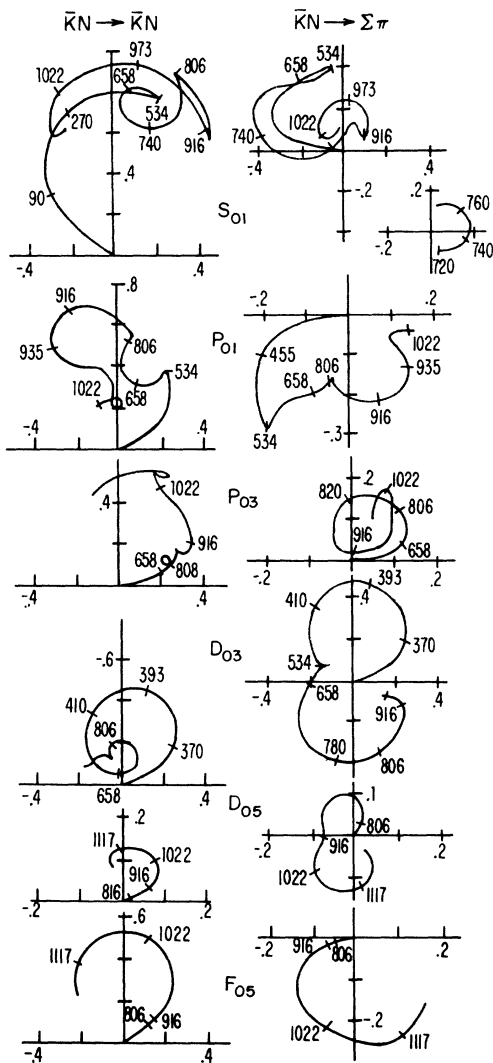


FIG. 1. The $I=0$ partial-wave amplitudes of the two reactions $\bar{K}N \rightarrow \bar{K}N$ and $\bar{K}N \rightarrow \Sigma\pi$ are shown in the Argand diagrams.

tal data on the elastic scattering in the polarized target. The P_{01} amplitudes seem to resonate twice. The resonant effect at 920 MeV/c with a mass of 1755 MeV is clearly seen both in the $\bar{K}N$ and $\Sigma\pi$ channels. The effect at 520 MeV/c with a mass of 1570 MeV is not clear but the K matrix has a pole at this energy. The P_{03} amplitude shows the small resonant loop in the $\Sigma\pi$ channel at 820 MeV/c but its coupling to the $\bar{K}N$ channel is very weak. This could be a possible resonant effect with a mass of 1710 MeV. The D_{03} amplitudes resonate twice, both at the masses of the well-known resonance $Y_0^*(1520)$ and $Y_0^*(1690)$. The resonance parameters obtained from this analysis for the $Y_0^*(1520)$ agree very well with

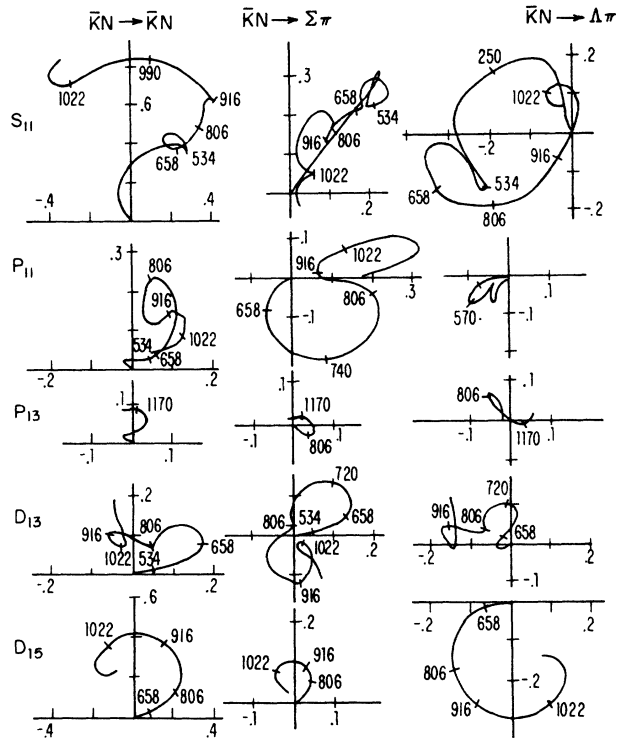


FIG. 2. The $I=1$ partial-wave amplitudes of the three reactions $\bar{K}N \rightarrow \bar{K}N$, $\bar{K}N \rightarrow \Sigma\pi$, and $\bar{K}N \rightarrow \Lambda\pi$ are shown in the Argand diagrams.

the Berkeley table¹⁵ value. However, the branching ratios of $Y_0^*(1690)$ obtained from this analysis are noticeably different from the table values. The branching ratio into the $\Sigma\pi$ channel is much larger and the three-body decay mode is very small. The D_{05} amplitudes resonate clearly at 1080 MeV/c and these also show some resonant effect mainly in the $\Sigma\pi$ channel at 840 MeV/c. The F_{05} amplitudes resonate clearly at the location of the well-known resonance $Y_0^*(1815)$ and the branching ratios are in good agreement with the accepted values.

The Argand diagrams of the reaction amplitudes in the total isospin-1 channel are shown in Fig. 2. The S_{11} amplitudes first resonate at 620 MeV/c with small elasticity and this resonance mainly branches into the $\Lambda\pi$ channel. Next this wave resonates again at 990 MeV/c, this time mainly into the elastic $\bar{K}N$ channel. At both of these momenta, the small loops in the $\Sigma\pi$ channels are also seen. The P_{11} amplitudes have a very strong resonant effect in the $\Sigma\pi$ channel and also have a sizable half-loop in the $\bar{K}N$ channel, both at the momentum of 740 MeV/c. The P_{13} amplitudes are in general very weak and do not indicate any resonant structure. The D_{13} amplitudes also resonate at a momentum of 740 MeV/c

TABLE I. The resonance parameters obtained from the multichannel phase-shift analysis. E_R is the resonant energy in MeV and Γ is the width of the resonance in MeV. χ_{AB} is the branching ratio where AB indicates the decay channel. Comments indicate the status of the resonances.

| Partial Waves | E_R | Γ | $\chi_{\bar{K}N}$ | $\chi_{\Sigma\pi}$ | $\chi_{\Lambda\pi}$ | χ_3 body | Comments |
|-----------------|-------|----------|-------------------|--------------------|---------------------|----------------------|-----------------------------------|
| S ₀₁ | 1670 | 35 | .28 | .52 | - | .20($\Lambda\eta$) | Established |
| | 1780 | 40 | .80 | .07 | - | .13 | Previously suggested ^a |
| S ₁₁ | 1620 | 40 | .05 | .13 | .46 | .36 | New ^b |
| | 1790 | 50 | .80 | .03 | .01 | .16 | Established ^c |
| P ₀₁ | 1570 | 50 | Seen | Seen | - | - | Possible (New) |
| | 1755 | 35 | .30 | .10 | - | .60 | Previously suggested ^d |
| P ₁₁ | 1670 | 50 | .14 | .42 | .00 | .44 | New ^e |
| P ₀₃ | 1710 | 20 | Small | Seen | - | - | Possible (New) |
| D ₀₃ | 1519 | 16 | .45 | .46 | - | .09 | Established |
| | 1690 | 55 | .22 | .73 | - | .05 | Established |
| D ₁₃ | 1670 | 40 | .07 | .32 | .08 | .53 | Established |
| D ₀₅ | 1720 | 20 | Small | Seen | - | - | Possible (New) |
| | 1830 | 80 | .24 | .09 | - | .67 | Established |
| D ₁₅ | 1765 | 100 | .42 | .02 | .22 | .34 | Established |
| F ₀₅ | 1810 | 70 | .52 | .13 | - | .35 | Established |
| F ₁₅ | 1910 | 60 | .07 | .25 | .10 | .58 | Fixed (Breit-Wigner) |

^a Refs. 11 and 13 observed independently.

^b There has been previous evidence for a resonance of this mass, width, and branching but of unknown spin and parity observed in production experiment. See Ref. 14.

^c The $\bar{K}N$ branching-ratio value is very different from that given in Ref. 15.

^d Ref. 1.

^e Previous evidence suggested a resonance about 100 MeV lower in energy. See Ref. 1.

c. Both resonances at a mass of 1670 MeV in P_{11} and D_{13} partial waves have very similar resonance parameters. The D_{15} partial waves resonate very strongly at the location of the well-known resonance $Y_0^*(1765)$ and the branching ratios are in general in good agreement with the accepted values, except that the $\Lambda\pi$ branching ratio is somewhat larger than the value given by the Berkeley table.¹⁵

The summary of the resonance parameters obtained from this multichannel analysis is given in Table I. The following two conditions are used in determining the resonant character of the partial waves. (a) The resonant amplitude should describe a good portion of a circle in the Argand diagram and the speed of the amplitude as a function of energy should pass through a maximum. (b) The K matrix should have a pole near the resonant energy and one of the eigenphases should pass through $\frac{1}{2}\pi$. Only those partial waves which satisfy these two conditions are listed in this table as resonances. In determining the resonance parameters, all the following three methods have been used: superposition of

a best half-circle on the Argand diagrams, speed criterion, and the diagonalization of the K matrix. The resonance parameters given in Table I are the averages of these three separate estimates. The Comments column of the table indicates the present status of these resonances. The following concluding remarks can be made: The $\bar{K}N$ system is very rich with hyperon resonances, and much more data are needed to do this type of analysis more conclusively.

It is a great pleasure to acknowledge the support and encouragement of Professor J. C. Street and Professor R. Wilson.

*Work supported by the U. S. Atomic Energy Commission.

¹R. Armenteros *et al.*, Nucl. Phys. **B8**, 183, 195, 223, 233 (1968), and **B14**, 91 (1969), and **B21**, 15 (1970), and in *Hyperon Resonances—70*, edited by E. C. Fowler (Moore, Durham, N. C., 1970), p. 123.

²B. Conforto *et al.*, Nucl. Phys. **B8**, 265 (1968), and to be published.

³D. Berley *et al.*, Phys. Rev. Lett. **15**, 641 (1965), and **16**, 162(E) (1966); L. Bertanza *et al.*, Phys. Rev.

177, 2036 (1969); D. Berley *et al.*, to be published.

⁴D. Berley *et al.*, Phys. Rev. D 1, 1966 (1970), and 3, 2297 (1971); J. Wong and W. Willis, Bull. Amer. Phys. Soc. 14, 592 (1969); J. Wong, thesis, Yale University, 1969 (unpublished).

⁵R. Levi Setti, in *Proceedings of the Lund International Conference on Elementary Particles*, edited by G. von Dardel (Berlingska Boktryckeriet, Lund, Sweden, 1970), p. 339; R. D. Tripp, in *Hyperon Resonances—70*, edited by E. C. Fowler (Moore, Durham, N. C., 1970), p. 95.

⁶See J. K. Kim, Phys. Rev. Lett. 19, 1074 (1967) for the data used.

⁷D. V. Bugg *et al.*, Phys. Rev. 168, 1466 (1968); R. Armenteros *et al.*, Nucl. Phys. B21, 15 (1970).

⁸S. Andersson-Almehed *et al.*, Nucl. Phys. B21, 515

(1970).

⁹M. Ross and G. Shaw, Ann. Phys. (New York) 13, 147 (1961).

¹⁰Kim Ref. 6.

¹¹J. K. Kim, in *Hyperon Resonances—70*, edited by E. C. Fowler (Moore, Durham, N. C., 1970), p. 161; N. P. Samios, in Proceedings of the Fifteenth International Conference on High Energy Physics, Kiev, U. S. S. R., 1970 (Atomizdat., Moscow, to be published).

¹²A. H. Rosenfeld and W. L. Humphrey, Annu. Rev. Nucl. Sci. 13, 103 (1963); J. P. Chandler, unpublished.

¹³C. Bricman, M. Ferro-Luzzi, and J. P. Lagnaux, Phys. Lett. 33B, 511 (1970).

¹⁴D. J. Crennell *et al.*, Phys. Rev. Lett. 21, 648 (1968).

¹⁵M. Roos *et al.*, Phys. Lett. 33B, 1 (1970).